JPP JOURNAL OF Pharmacy and Pharmacology
ROYAL PHARMACEUTICAL SOCIETY
JPP Journal of Pharmacy And Pharmacology
Research Paper

Development of a direct contact astrocyte-human cerebral microvessel endothelial cells blood–brain barrier coculture model

Chris Kulczar[a], Kelsey E. Lubin[a], Sylvia Lefebvre[a], Donald W. Miller[b] and Gregory T. Knipp[a]

[a]Department of Industrial and Physical Pharmacy, College of Pharmacy, Purdue University, West Lafayette, IN, USA and [b]Department of Pharmacology & Therapeutics, University of Manitoba, Winnipeg, MB, Canada

Keywords
blood–brain barrier coculture; human cerebral microvessel endothelial cells; human astrocytes; paracellular permeability

Correspondence
Gregory T. Knipp, Department of Industrial and Physical Pharmacy, College of Pharmacy, Purdue University, 575 Stadium Mall Dr., West Lafayette, IN 47907-2091, USA.
E-mail: gknipp@purdue.edu

Received November 23, 2016
Accepted July 1, 2017

doi: 10.1111/jphp.12803

Abstract

Objectives In conventional in-vitro blood–brain barrier (BBB) models, primary and immortalized brain microvessel endothelial cell (BMEC) lines are often cultured in a monolayer or indirect coculture or triculture configurations with astrocytes or pericytes, for screening permeation of therapeutic or potentially neurotoxic compounds. In each of these cases, the physiological relevancy associated with the direct contact between the BMECs, pericytes and astrocytes that form the BBB and resulting synergistic interactions are lost. We look to overcome this limitation with a direct contact coculture model.

Methods We established and optimized a direct interaction coculture system where primary human astrocytes are cultured on the apical surface of a Transwell® filter support and then human cerebral microvessel endothelial cells (hCMEC/D3) seeded directly on the astrocyte lawn.

Key findings The studies suggest the direct coculture model may provide a more restrictive and physiologically relevant model through a significant reduction in paracellular transport of model compounds in comparison with monoculture and indirect coculture. In comparison with existing methods, the indirect coculture and monoculture models utilized may limit cell–cell signaling between human astrocytes and BMECs that are possible with direct configurations.

Conclusions Paracellular permeability reductions with the direct coculture system may enhance therapeutic agent and potential neurotoxicant screening for BBB permeability better than the currently available monoculture and indirect coculture in-vitro models.

Introduction

The blood–brain barrier (BBB) is a highly restrictive barrier between the systemic circulation and the brain parenchyma.[1–5] The BBB functions to exclude harmful xenobiotics while permitting the entry of nutrients and removal of waste allowing for a neuronal environment optimal for development and function.[6–8] One of the key elements of the BBB is a continuous endothelium with the presence of exceedingly restrictive tight junctions between brain microvessel endothelial cells. These tight junctions prevent the paracellular movement of hydrophilic molecules and ions to a greater extent than anywhere else in the body.[9,10] This restriction is believed to be due, in part, to an increased expression of claudins 3, 5 and 12 in brain microvessel endothelial cells compared with microvessel endothelial cells in the periphery.[11] In addition to tight junctions, BBB endothelial cells also express a number of drug-metabolizing enzymes, such as cytochrome P450 enzymes (CYP450), and efflux transporters, such as P-glycoprotein (P-gp) and breast cancer resistance protein (BCRP), which act to efflux xenobiotics moving transcellularly.[12–14]

Further investigation of the *in-vivo* BBB reveals supporting cells, such as astrocytes and pericytes, which form a symbiotic, synergistic relationship with BMECs that significantly enhances the barrier properties.[3,15,16] Due to their close-knit interactions leading to BBB formation, the

collection of endothelial cells, astrocytes and pericytes was coined the neurovascular unit. Each of the cells play a role in creation of the barrier, and while tight junctions between the endothelial cells are responsible for the barrier function itself, the astrocytes and pericytes are thought to be necessary for co-differentiation with the endothelial cells promoting this BBB phenotype.[17] Among other things, astrocytes are believed to be responsible for regulating the development of tight junctions, the movement of water and glucose across the BBB, metabolism and the localization of transporters.[2] In addition, astrocytes highly express CYP450 enzymes and may serve an important neuroprotective role by metabolizing and removing many xenobiotics, including pharmaceutical compounds.[18] Pericytes, on the other hand, are thought to be important for the production of soluble growth factors as well as production and maintenance of an extracellular matrix rich in collagen, fibronectin, proteoglycans and laminin that is important for integrity of the BBB and may be important for proper BBB differentiation.[19–21]

Due to the increasing importance of translatable knowledge established by understanding the properties required for traversing the BBB, a number of different *in-vitro* permeability screening models have been established.[8,17,22–32] Most of these models utilize primary human or animal BMECs.[33] While primary human BMECs may provide the most ideal and relevant model, the availability of such tissues is minimal, reducing their utility for high-throughput screening.[6] Due to the lack of available healthy human brain specimens, many attempts have been made to use animal brain BMEC isolates as a surrogate. These cells are often of murine, bovine or porcine origin. Primary cells of animal origin have been shown to provide relatively high transendothelial electrical resistance (TEER) indicative of the presence of developed tight junctions.[25,29,31,34] However, one must question the physiological relevance of these models for drug screening, especially based on species differences including non-paracellular routes of permeation indicative of the vast majority of BBB-permeable compounds. Therefore, new models have been established making use of immortalized human tissues which provide the relevance of a human cell line without the disadvantage of short supply.

One of the most often used immortalized human BMEC cell lines is the human cerebral microvessel endothelial (hCMEC/D3) cell line. The hCMEC/D3 cell line was established through hTERT and SV40 large T antigen immortalization of endothelial cells isolated from microvessels of a human temporal lobe.[35] hCMEC/D3 cultures form monolayers on collagen-coated surfaces and are contact inhibited lending themselves to high-throughput Transwell® permeation studies. Analysis of the cell line has shown similarities in morphology and protein expression between hCMEC/D3s and primary human BMECs. However, hCMEC/D3s do not appear to form restrictive tight junctions consistent with those found *in vivo*, reaching TEER values of only 30–50 $\Omega \times cm^2$ compared with TEER values of over 1000 $\Omega \times cm^2$ *in vivo* in other species including the frog.[8,32,35–37] These leaky tight junctions may allow paracellular movement of compounds that permeate by the transcellular route *in vivo*, leading to irrelevant permeability values. While optimization of culture conditions, for example media, density, cell source, has led to modest increases in monoculture TEER, these values are still well below those seen *in vivo*.[6,38]

Due to the leakiness of these monocultures, many groups have examined methods for reducing the paracellular permeability of these models. One approach is to use astrocyte conditioned media.[39] In these studies, soluble factors released by the astrocytes were able to interact with BMECs to create a more *in-vivo*-like environment that lead to enhanced differentiation and reduced paracellular permeability. However, for hCMEC/D3 cultures, non-significant changes were seen in TEER when using astrocyte conditioned media.[27,35] Instead, the most significant reductions in paracellular permeability were seen when astrocytes were grown on the basolateral side of the filter or on the plastic well plate surface in the same Transwell® as the hCMEC/D3s (Figure 1a).[8,32] While a reduction in paracellular permeability of marker compounds and increases in TEER were seen for both of these conditions, greater changes were observed in cells grown on the basolateral side of the Transwell®.[6] These models are likely more physiologically relevant due to the symbiotic signalling and differentiation that is able to occur when both cell types are grown in the same culture. In addition, the increased tightness seen when growing astrocytes on the basolateral side of the Transwell® may reflect a closer proximity of astrocytic-released factors to endothelial cells, thus producing a greater response through reduced dilution.[28] Moreover, it is thought that the model in which cells are grown on the bottom of the Transwell®-permeable support may lead to tighter junctions due to the ability of the astrocytic endfeet to migrate through the pores of the filter and interact with the BMECs through direct contact. However, it should be noted that migration through Transwell® supports, especially through 0.4-μm pores which best support endothelial cell culture, is infrequent.[34,40]

It is apparent from the studies mentioned above and analysis of the neurovascular unit that the interplay between BMECs and astrocytes may serve an important role in differentiation of BMECs into providing a BBB phenotype. In addition, these studies have shown the proximity of the astrocytes and BMECs may be crucial.[2,28,40] However, the methods described in previous coculture models entail separating BMECs and astrocytes by a filter support

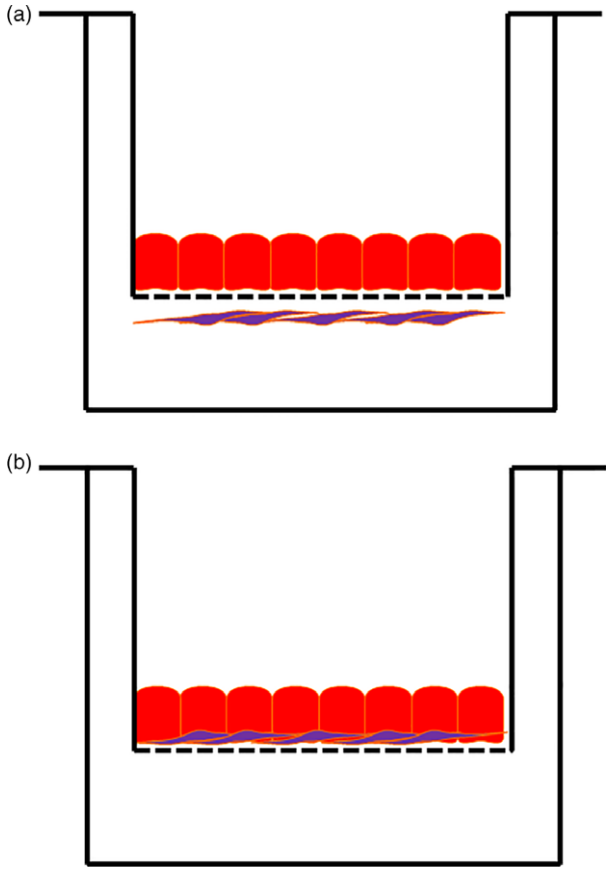

Figure 1 Past (indirect) vs current direct contact coculture models. (a) previous direct contact coculture model with BMEC and astrocytes separated by Transwell®-permeable filter support. (b) current direct contact coculture model, with BMEC and astrocytes in direct cell–cell contact. BMEC and astrocytes are shown in red and purple, respectively. [Color figure can be viewed at wileyonlinelibrary.com]

and in most cases a thick extracellular matrix. While the Transwell® support is often depicted to be thin in cartoon representations, the filter is approximately 10 μm thick and may represent a significant barrier to cell–cell interactions. It is hypothesized that removing this obstruction and allowing direct cell–cell contact may better enable direct symbiotic signalling and differentiation to occur, which in turn may lead to further reduction in paracellular permeability and a more *in-vivo* relevant model. An illustration of the model is shown in Figure 1b. To our knowledge, this is the first study to investigate changes in the human BMEC barrier properties when grown in direct contact with astrocytes. In addition, this study provides evidence that direct contact may provide additional benefit to the physiological relevance of BBB permeability models, particularly in restriction of paracellular permeability which has long hindered the use of immortalized BMECs in drug permeability screening. The results of these studies should facilitate additional research that aims at delineating phenotypic differences between the direct contact method used here and the filter-separated methods that are more commonplace.

Materials and Methods

Materials

Trypsin, phosphate-buffered saline (PBS), penicillin/streptomycin, type I rat tail collagen, poly-L-lysine, HEPES (4-(2-hydroxyethyl)-1-piperazineethanesulfonic acid) buffer, fibronectin, Maxgel™, Hank's balanced salt solution (HBSS), hydrocortisone, human basic fibroblast growth factor (bFGF), ascorbic acid, fetal bovine serum (FBS), MaxGel, lithium chloride, rhodamine-123 and verapamil were purchased from Sigma-Aldrich Company (St. Louis, MO, USA). EBM-2 growth media were manufactured by Lonza Group (Walkersville, MD, USA). Lipid concentrate was obtained from BD Biosciences (Sparks, MD, USA). 0.4-μm Transwell® 12-well plates and T75 flasks were made by Corning Lifesciences (Corning, NY, USA). Radiolabelled compounds were purchased from Moravek Biochemicals Inc. (Brea, CA, USA). MTT was obtained from RPI (Mount Prospect, IL, USA). The hCMEC/D3 cell line was graciously provided by Dr. Pierre Couraud of the Université Rene Descartes (Paris, France), while human astrocytes, human astrocyte media and astrocyte growth factor were obtained from ScienCell Research Laboratories (Carlsbad, CA, USA).

Cell culture

The hCMEC/D3 cells were cultured in EBM-2 supplemented with FBS, penicillin/streptomycin, bFGF, hydrocortisone, ascorbic acid, lipid concentrate and HEPES buffer. Cells were maintained in a 5% environment at 37 °C. HCMEC/D3 cells were passaged when confluence reached approximately 80%, at which time trypsinized cells were placed in a precollagenated (type I) flask. Media were changed every other day. Human astrocytes were cultured under similar conditions in human astrocyte media supplemented with FBS, astrocyte growth factor and penicillin/streptomycin. Cells were passaged approximately every 5 days into flasks precoated with poly-L-lysine.

Monoculture studies

In hCMEC/D3 monocultures, cells were seeded at a density of 1×10^5 cells/cm^2 on Corning Costar 12-well 0.4-μm polyester Transwells® pretreated with 65 μl of 1 mg/ml type I rat tail collagen and allowed to grow for 7 days. For human astrocyte monocultures, 4×10^4 cells were seeded onto Transwells® coated with 2 μg/cm^2 poly-L-lysine and grown for 9 days before conducting permeability studies.

Indirect coculture studies

Indirect coculture Transwells® were first pretreated with 65 μl of 1 mg/ml type I rat tail collagen in ethanol in the apical chamber and left to evaporate for 4 h. Following evaporation, the Transwells® were flipped and 2 μg/cm^2 poly-L-lysine was added to the basolateral side of the Transwells® and left overnight. Human astrocytes were plated on the basolateral side of the flipped Transwells® at a density of 4×10^4 cells/cm^2 and left to attach for 4 h. Transwells® were then placed into the normal orientation and grown for 48 h. After this time, hCMEC/D3 cells were plated in the apical compartment at a density of 1×10^5 cells/cm^2. The coculture was left to proliferate/differentiate in EBM-2 for an additional 7 days with media changes every other day before the permeability studies were conducted.

Direct coculture studies

For direct coculture studies, Transwell® inserts were coated with 2 μg/cm^2 poly-L-lysine and left overnight. Human astrocytes were then plated at a density of 4×10^4 cells/cm^2. Astrocytes were allowed to proliferate/differentiate for 48 h in astrocyte media. After 48 h, media were removed and hCMEC/D3s were plated in EBM-2 at a density of 1×10^5 cells/cm^2. The coculture was grown in EBM-2 with media changes every other day for an additional 7 days before studies were conducted.

Direct coculture optimization

Optimization of the direct coculture was studied separately by utilizing a number of media additives at varying concentrations. Hydrocortisone was studied at 1.4 μM and 100 nM, while lithium chloride was studied separately at 0–10 mM, each at the start of hCMEC/D3 seeding or at Day 2 and maintained throughout culturing. The impact of HEPES concentration in media was observed utilizing 10–50 mM concentrations upon the start of hCMEC/D3 plating. All culture conditions were the same as stated above throughout optimization. Degree of optimization was tested utilizing [C14]-mannitol as a paracellular marker, with permeability studies performed as stated below.

Cell viability assay

Cell viability in the presence of various HEPES concentrations was inferred by the mitochondrial oxidation of 3-(4,5-dimethylthiazol-2-yl)-2,5-diphenyltetrazolium bromide (MTT) dye. The direct contact coculture was plated in a 96-well plate following the same methods as stated above. On Day 7 post-hCMEC/D3 plating, media containing HEPES were removed and replaced with 190 μl fresh media and 10 μl of 5 mg/ml MTT and incubated at 37 °C with 5% CO_2 for 4 h. MTT was then removed and replaced with 200 μl DMSO and left agitating at room temperature for 1 h. Absorbance at 570 nm was determined using a plate reader. Cell viability was normalized to 10 mM HEPES control. Assays were performed with $n = 6$.

Permeability studies

Permeability studies were performed at 37 °C on a rocker plate in triplicate using [C14]-labelled markers ([C14]-urea, [C14]-mannitol, [C14]-sucrose, [C14]-inulin, [C14]-PEG-4000 and [C14]-propranolol) at a concentration of 0.25 μCi/ml in HBSS. In all studies, human astrocytes ranged from passages 6 to 12, while hCMEC/D3 cells ranged from passages 36 to 48. Before conducting all permeability studies, cells were washed twice with PBS before equilibrating in HBSS for 20 min shortly before the study. After study initiation, 100 μl of samples was taken at 15-, 30-, 45-, 60-, and 90-min time points. 4 ml of scintillation cocktail was added for analysis by scintillation counting. Permeability coefficients (cm/s) were obtained through the following equation:

$$P_{\text{apparent}} = \frac{\frac{dM}{dt}}{C_0 * SA * 60},$$

where $\frac{dM}{dt}$ is the rate of radionucleotide transfer across the cell layer, C_0 is the initial donor concentration, SA is the surface area of the Transwell® filter support, and 60 represents a correction factor from minutes to seconds.

Functional efflux

Monoculture and coculture cells were plated on a 96-well plate to assess cellular accumulation of rhodamine 123. Studies were performed at 37 °C on a rocking platform. Cells were incubated with 5 μM rhodamine 123 in HBSS for 1 h. Inhibition studies were performed by first preincubating cells with 10 μM verapamil in HBSS for 30 min at 37 °C. Cells were then incubated with both substrate and inhibitor for 1 h. Following 1-h incubation, cells were washed with PBS and lysed with buffer containing 20 mM Tris, 100 mM NaCl, 1 mM EDTA and 1% Triton X-100. Samples were analysed by measuring fluorescence with an excitation of 485 nm and emission of 535 nm using a plate reader. All experiments were conducted in triplicate ($n = 3$).

Statistics

The distribution of permeability coefficients across the brain has not been well studied; however, some studies involving other membranes suggest that permeability can be normally or log-normally distributed based on the compound.[41,42] Therefore, the data presented here have been

subjected to both parametric and nonparametric tests. Studies were compared using the Mann–Whitney test or the Kruskal–Wallis test with a Dunn's post-hoc test. Additionally, all studies were also subjected to a two-tailed unpaired Student's *t*-test or one-way ANOVA with a Bonferroni post-hoc test. Studies with *P*-values less than 0.05 were considered to have significant differences.

Results

Cell culture optimization

To delineate changes in BBB phenotype upon hCMEC/D3 coculture with human astrocytes, permeability was measured with a number of marker compounds. The hCMEC/D3 monoculture cells and the indirect coculture models were used for comparison. However, the direct coculture model was first optimized for minimal paracellular permeability.

Hydrocortisone was utilized as a media additive due to its endogenous role as an anti-inflammatory agent that increases tight junctional integrity.[43] Permeability studies were conducted using 1.4 μM and 100 nM at the start of hCMEC/D3 culture or after 2 days of proliferation. Results in Figure 2a showed that 1.4 μM hydrocortisone at the start of hCMEC/D3 plating provided the lowest [^{14}C]-mannitol permeability compared with 100 nM ($1.54 \pm 0.07 \times 10^{-5}$ and $3.56 \pm 0.29 \times 10^{-5}$ cm/s; *t*-test, $P = 0.005$; Mann–Whitney, $P = 0.100$).

Lithium chloride was selected as a media additive because of its implications in the Wnt/β-catenin pathway and because it increases tight junctional protein expression.[44,45] LiCl, at a concentration of 10 mM, was added to media at the start of hCMEC/D3 plating or 2 days after. Results in Figure 2b showed that LiCl addition at the start of plating and at Day 2 both increased [^{14}C]-mannitol permeability compared with no LiCl addition ($2.20 \pm 0.18 \times 10^{-5}$, $1.97 \pm 0.12 \times 10^{-5}$ and $1.52 \pm 0.07 \times 10^{-5}$ cm/s; one-way ANOVA Bonferroni, $P = 0.036$ and $P = 0.028$; Kruskal–Wallis Dunn's test, $P = 0.408$ and $P = 0.034$).

The hCMEC/D3 cell line has been shown to be sensitive to small changes in pH; therefore, HEPES concentration was optimized to limit pH changes during cell culturing.[46] HEPES was studied at 10, 25, and 50 mM on both the direct coculture and hCMEC/D3 monolayers. The direct coculture was found to be less permeable than hCMCEC/D3 monolayers at all HEPES concentrations with 25 mM showing the best results for decreased permeability of [^{14}C]-mannitol and minimal toxicity for the direct coculture ($1.28 \pm 0.07 \times 10^{-5}$ cm/s; *t*-test, $P = 0.033$; Mann–Whitney, $P = 0.100$) as seen in Figure 2c. MTT assay results showed an insignificant reduction in cell viability ($-8.2 \pm 2.0\%$; $P > 0.05$) for 25 mM HEPES sample in comparison with 10 mM HEPES. A HEPES concentration of 50 mM resulted in a significant decrease in cell viability ($-28.4 \pm 2.6\%$; one-way ANOVA Bonferroni, $P = 0.00003$; Kruskal–Wallis Dunn's test, $P = 0.001$) when compared with a 10 mM HEPES control (data not shown).

An extensive design of experiments (DOE) was used for optimization of hCMEC/D3 and astrocyte seeding density, basement matrix, media additives and seeding time before conducting the following studies. These attributes were assessed using TEER and paracellular permeability markers with all studies performed in triplicate. Results of the optimization are shown in Table 1.

Paracellular permeability

Direct contact coculture

As noted above, the hCMEC/D3 cell line, while tighter than other immortalized human BMEC cells, possess tight junctions that lack ideal physiological relevance. To investigate changes in tight junction pore radius, five marker compounds of varying hydrodynamic radii were used to determine changes in paracellular permeability. As expected, increases in hydrodynamic radii lead to decreased apparent permeability coefficients for paracellular markers. However, the extent of changes in permeability varied between monoculture and coculture, likely due to the effects predicted by the Renkin molecular sieving function as the pore radii approach the size of the sieved molecule.[31,36,47,48] Though, it should be noted that in the presence of astrocytes, the assumptions made by the Renkin function including the presence of a single pore varied and increased tortuosity and porosity exist. Thus, the effects of permeation across the astrocytes cannot be easily corrected to obtain a pore radius.

As shown in Figure 3, decreases in paracellular permeability from the monoculture and coculture were seen for [^{14}C]-urea ($2.96 \pm 0.11 \times 10^{-5}$ and $2.43 \pm 0.15 \times 10^{-5}$ cm/s; *t*-test, $P = 0.030$; Mann–Whitney, $P = 0.100$), [^{14}C]-mannitol ($1.98 \pm 0.05 \times 10^{-5}$ and $1.52 \pm 0.07 \times 10^{-5}$ cm/s; *t*-test, $P = 0.001$; Mann–Whitney, $P = 0.100$), [^{14}C]-sucrose ($1.52 \pm 0.13 \times 10^{-5}$ and $1.17 \pm 0.008 \times 10^{-5}$ cm/s; *t*-test, $P = 0.044$; Mann–Whitney, $P = 0.100$) and [^{14}C]-inulin ($8.46 \pm 0.02 \times 10^{-6}$ and $7.55 \pm 0.3 \times 10^{-6}$ cm/s; *t*-test, $P = 0.034$; Mann–Whitney, $P = 0.100$), respectively. The smallest decrease was seen for [^{14}C]-PEG-4000 ($3.93 \pm 0.36 \times 10^{-6}$ and $3.57 \pm 0.10 \times 10^{-6}$ cm/s; *t*-test, $P = 0.227$; Mann–Whitney, $P = 0.100$).

The direct contact coculture was assessed for reproducibility by repeating paracellular permeability experiments using [^{14}C]-inulin as a marker. As shown in Figure 4, [^{14}C]-inulin permeability was performed in two additional independent experiments ($7.51 \pm 0.01 \times 10^{-6}$

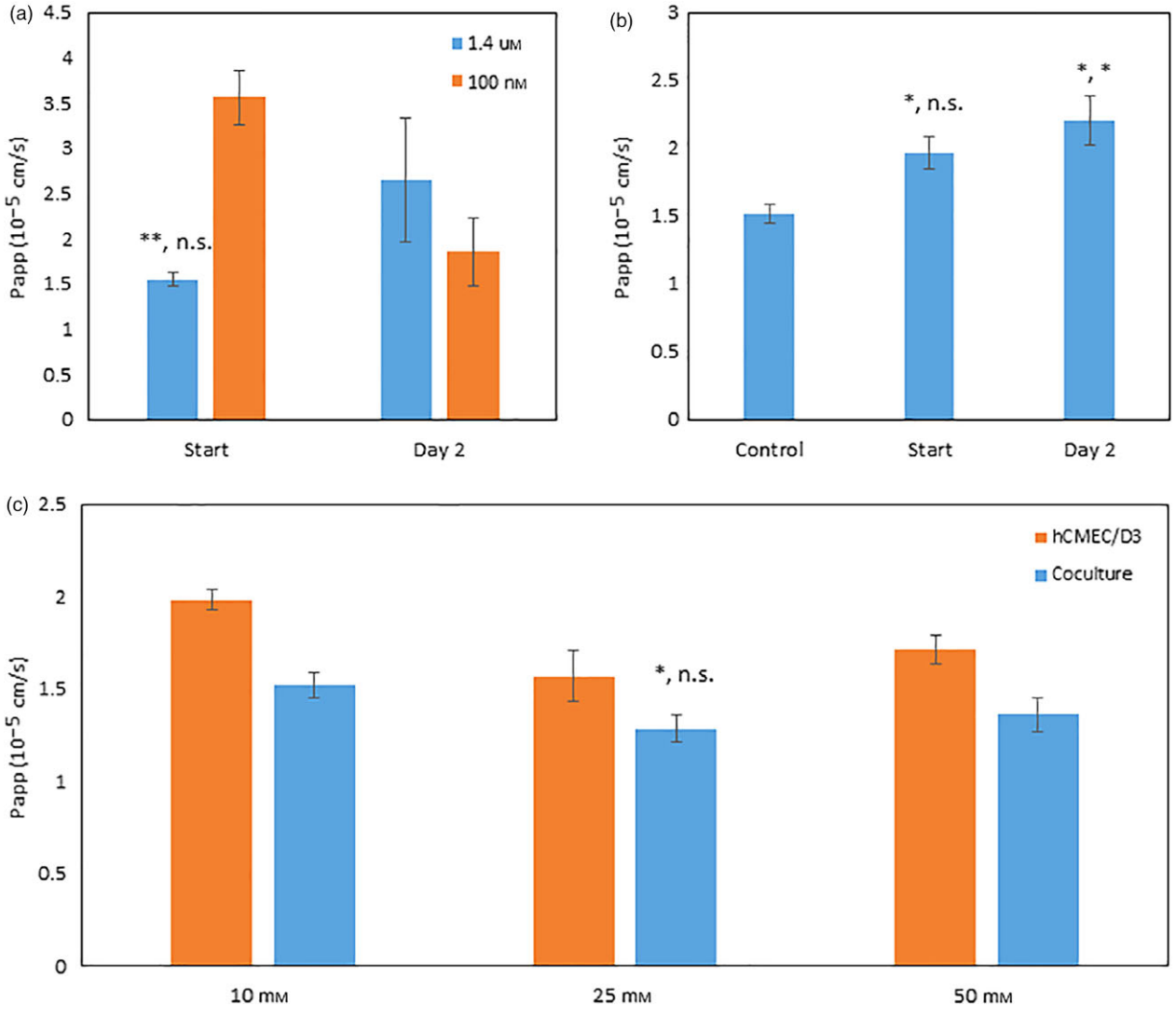

Figure 2 Optimization of direct contact culture using apparent permeability of [^{14}C]-mannitol. (a) Hydrocortisone added to media at 1.4 μM or 100 nM at the start of human cerebral microvessel endothelial cells plating or 2 days postplating. (b) Lithium chloride at 10 mM compared with control (0 mM) when added at the start of human cerebral microvessel endothelial cells plating or 2 days postplating. (c) 4-(2-hydroxyethyl)-1-piperazineethanesulfonic acid concentrations of 10, 25 and 50 mM added to media for human cerebral microvessel endothelial cells monolayer in comparison with direct culture. Studies were run in triplicate and subjected to Student's *t*-test and Mann–Whitney test (a and c) or one-way ANOVA with Bonferroni post-hoc test or Kruskal–Wallis with Dunn's post-hoc test (b). Significant changes are noted with an asterisk (*) for $P < 0.05$ and (**) for $P < 0.01$. Significant levels are reported as (*t*-test, MW) or (one-way ANOVA, KW). Error bars represent 1 standard deviation ($n = 3$). [Color figure can be viewed at wileyonlinelibrary.com]

and $7.94 \pm 0.03 \times 10^{-6}$ cm/s; one-way ANOVA, $P = 0.067$; Kruskal–Wallis, $P = 0.021$, Dunn's test, $P = 0.036$) with cells cultured at different passage numbers.

Indirect contact coculture

It is well established that changes in culture conditions and cell source can cause significant changes in protein expression of drug-metabolizing enzymes, efflux proteins, etc., which are the focus of ongoing studies.[49,50] In addition, modifications in media have been shown to have considerable effects on BMEC differentiation and tight junction formation.[32,51,52] To establish an internal laboratory control, an indirect coculture model was also run to investigate differences in paracellular permeability when culturing human astrocytes in direct contact with hCMEC/D3 cells.[6,38] Figure 5 shows that direct contact leads to a reduction in permeation compared with indirect contact of both [^{14}C]-mannitol ($1.52 \pm 0.07 \times 10^{-5}$ and $1.89 \pm 0.15 \times 10^{-5}$ cm/s; *t*-test, $P = 0.038$; Mann–Whitney,

Table 1 Optimization of the direct contact coculture model

Attributes	Range	Optimized value
hCMEC/D3 seeding density	50 000–250 000 cells/cm^2	100 000 cells/cm^2
Astrocyte seeding density	10 000–40 000 cells/cm^2	40 000 cells/cm^2
Basement matrix	Collagen, poly-L-lysine, MaxGel, Fibronectin	Poly-L-lysine
Seeding time	3, 5, 7, 9, 11, 13, 15, 17, 19 Days	7 Days
Seeding order	Separate vs concurrent plating	Separate
Media	EBM-2 vs astrocyte medium	EBM-2
Fetal bovine serum	Serum vs serum-free	Serum
Hydrocortisone	100 nM–1.4 μM	1.4 μM
HEPES	10–50 mM	25 mM
Lithium chloride	0–10 mM	0 mM

$P = 0.100$) and [^{14}C]-sucrose ($1.17 \pm 0.008 \times 10^{-5}$ and $1.53 \pm 0.12 \times 10^{-5}$ cm/s; *t*-test, $P = 0.035$; Mann–Whitney, $P = 0.100$), respectively.

Passive transcellular permeability

To investigate the effects on transcellular permeation when culturing human astrocytes and hCMEC/D3 cells in direct contact, [^{14}C]-propranolol apparent permeability was measured. Due to its high lipophilicity, the majority of propranolol is uncharged at physiological pH and is presumed to have minimal paracellular permeation so it was selected as a marker for transcellular permeation. Figure 6 shows that insignificant changes in [^{14}C]-propranolol apparent permeability were seen between hCMEC/D3 and direct contact coculture ($1.91 \pm 0.19 \times 10^{-5}$ and $1.61 \pm 0.04 \times 10^{-5}$ cm/s). This may indicate transcellular permeation through hCMEC/D3 cells followed by passive transport across the human astrocyte layer which do not possess tight junctions. However, these values are nearly threefold lower than astrocytes grown in monoculture ($4.58 \pm 0.41 \times 10^{-5}$ cm/s). This makes it difficult to delineate the effect of astrocytes on transcellular permeation of [^{14}C]-propranolol across the hCMEC/D3 monolayer.

Functional efflux by cellular accumulation

The extent of functional efflux of P-gp in both the monoculture and direct contact coculture was assessed using P-gp substrate rhodamine 123 by measuring cellular accumulation in the presence and absence of an inhibitor, verapamil. As seen in Figure 7, the presence of verapamil increased total cellular accumulation in both monoculture and coculture models compared with the accumulations without inhibitor (monoculture, $2.8 \pm 1.6\%$ to $4.0 \pm 0.4\%$; *t*-test, $P = 0.258$; Mann–Whitney, $P = 0.400$; coculture, $1.2 \pm 1.0\%$ to $2.6 \pm 0.4\%$; *t*-test, $P = 0.068$; Mann–Whitney, $P = 0.100$). Although these data are not statistically significant ($P > 0.05$), the total accumulation of rhodamine 123 is greater in the hCMEC/D3 monoculture compared with the direct contact coculture.

Discussion

Previous research has demonstrated that the hCMEC/D3 cell line forms a barrier that is a functionally and physiologically relevant model for human BMECs. This is predicated on the fact that hCMEC/D3 cells possess a similar morphology and protein expression as found in primary human BMECs.[35,53] In addition, the immortalized cell line is of human origin, can be grown in monolayers and is contact inhibited, properties that all lend themselves for use

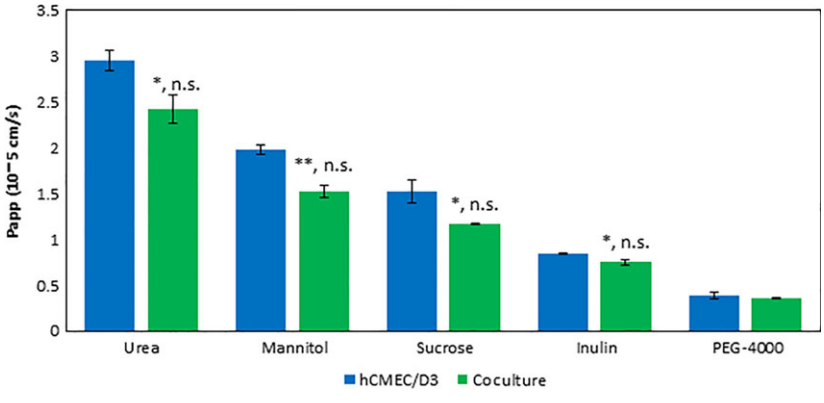

Figure 3 Apparent permeability for five paracellular [^{14}C]-labelled markers of various hydrodynamic radii. Studies were run in triplicate and subjected to Student's *t*-test or Mann–Whitney test. Significant changes are noted with an asterisk (*) for $P < 0.05$ and (**) for $P < 0.01$. Significant levels are reported as (*t*-test, MW). Error bars represent 1 standard deviation ($n = 3$). [Color figure can be viewed at wileyonlinelibrary.com]

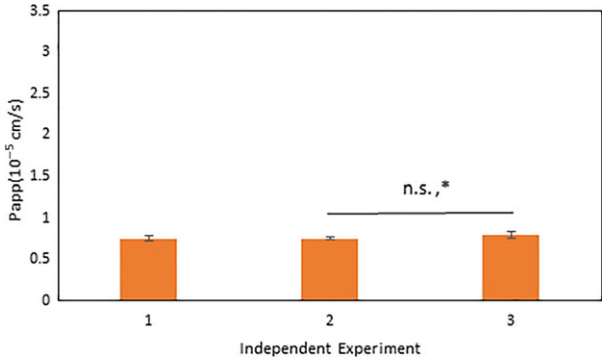

Figure 4 Apparent permeability of [^{14}C]-inulin, a paracellular marker, across the direct contact coculture. Studies were subjected to one-way ANOVA with a Bonferroni post-hoc test and Kruskal–Wallis with Dunn's post-hoc test. Significant changes are noted with an asterisk (*) for $P < 0.05$ and (**) for $P < 0.01$. Significant levels are reported as (one-way ANOVA, KW). Error bars represent 1 standard deviation ($n = 6$). [Color figure can be viewed at wileyonlinelibrary.com]

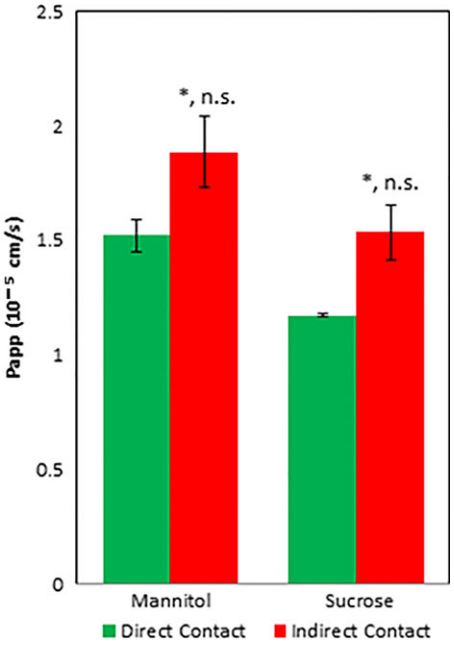

Figure 5 Apparent permeability of [^{14}C]-mannitol and [^{14}C]-sucrose across direct and indirect contact cocultures. Studies were run in triplicate and subjected to Student's *t*-test or Mann–Whitney test. Significant changes are noted with an asterisk (*) for $P < 0.05$. Significant levels are reported as (*t*-test, MW). Error bars represent 1 standard deviation ($n = 3$). [Color figure can be viewed at wileyonlinelibrary.com]

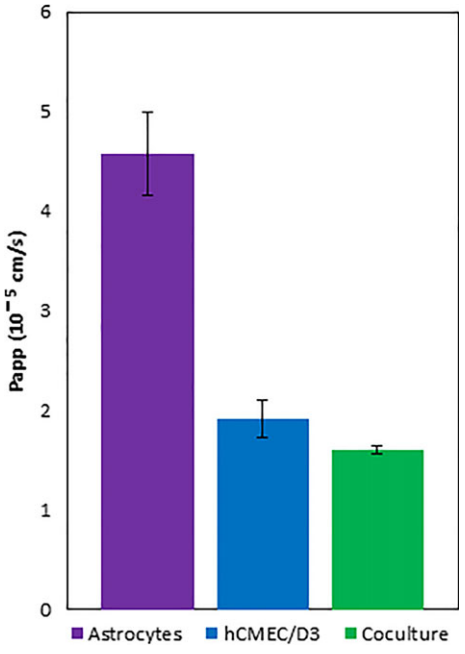

Figure 6 Apparent permeability of [^{14}C]-propranolol, a passive transcellular permeability marker. Studies were subjected to one-way ANOVA with a Bonferroni post-hoc test and Kruskal–Wallis with Dunn's post-hoc test. Non-significant changes ($P > 0.05$) were seen between monoculture and coculture. Error bars represent 1 standard deviation ($n = 3$). [Color figure can be viewed at wileyonlinelibrary.com]

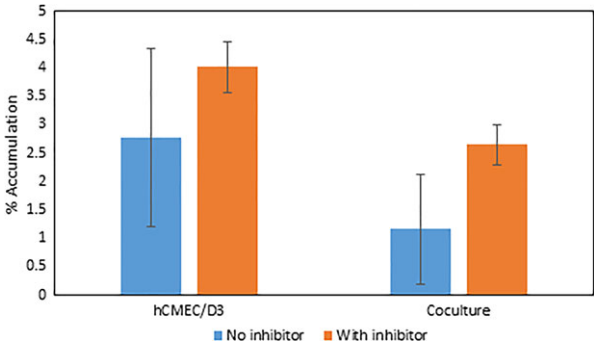

Figure 7 Total percentage of accumulation of rhodamine 123 to show functional expression of efflux transporter P-glycoprotein in human cerebral microvessel endothelial cells monoculture and direct contact coculture. Efflux of P-gp substrate rhodamine 123 was assessed in the presence and absence of P-gp inhibitor verapamil. Studies were subjected to one-way ANOVA with a Bonferroni post-hoc test and Kruskal–Wallis with Dunn's post-hoc test. No significant difference was observed between the presence and absence of inhibitor for either model ($P > 0.05$). Error bars represent 1 standard deviation ($n = 3$). [Color figure can be viewed at wileyonlinelibrary.com]

in *in-vitro* permeability screening.[32] However, hCMEC/D3 monolayers lack the tightness found *in vivo*, which may lead to increased paracellular permeation of drug molecules that in turn may obfuscate the ability to predict transcellular permeation that is observed when studying *in-vivo* brain distribution.[6] As has been previously shown, coculturing hCMEC/D3 cells with astrocytes has led to pronounced decreases in paracellular permeability for BMECs, which

may mitigate this problem.[54] Moreover, the presence of the astrocytes enables a more relevant understanding of the transport across the *in-vivo* neurovascular unit.

Since the discovery of the neurovascular unit, this interplay between BMECs and astrocytes at the BBB has been studied. While there are still unknowns, many of their interactions have been elucidated.[2,13,55,56] For BMECs, it has been shown that astrocytes play an important role in tight junction development, localization and expression of transporters, as well as upregulation of metabolic enzymes, which are currently being investigated.[32,35,56] In addition, some of these interactions may require symbiotic cross-talk leading to co-differentiation,[17,57] while some of these adaptations can be seen with an indirect coculture of BMECs with astrocytes *in vitro*; leakiness of the tight junctions is still significantly higher than in *in-vivo* conditions.[6] It is hypothesized that one reason for continued leakiness is an inability for astrocytes to form true direct contact with the BMECs in this model due to the presence of the Transwell®-permeable support. This lack of contact may hinder cross-talk between endothelial cells and astrocytes. For this reason, a direct contact model with hCMEC/D3 cells seeded directly onto human astrocytes was investigated.

An extensive amount of optimization was performed from investigating cell density and media compositional changes to increase barrier tightness of the direct coculture. Hydrocortisone was selected as a media additive because previous studies have shown that culturing with 50 nM hydrocortisone led to decreases in paracellular permeability and increases in tight junction protein expression.[43] This is thought to occur through the inhibition of tumour necrosis factor alpha (TNF-alpha) as TNF-alpha signalling can lead to tight junction breakdown.[43] A hydrocortisone concentration of 1.4 μM caused the larger decrease in [^{14}C]-mannitol paracellular permeability when added at the start of hCMEC/D3 plating compared with 100 nM of hydrocortisone. Lithium chloride at 10 mM showed no decrease in [^{14}C]-mannitol permeability when added at the start of hCMEC/D3 plating or 2 days postplating when compared with media without LiCl. LiCl was added 2 days postplating to allow cells to reach full confluency as LiCl is known to promote differentiation. As there was no significant decrease in paracellular permeability upon Day 2 LiCl addition, it was hypothesized that there may have been premature differentiation before cells reached full confluency. This would lead to an incomplete monolayer and a relatively leaky cell barrier. Longer LiCl exposure times may have been required and could not be ruled out. HEPES was utilized to maintain pH throughout culturing with 25 mM showing the best results for decreased permeability for the direct coculture compared with hCMEC/D3 monolayer. A slight increase in [^{14}C]-mannitol permeability was observed at 50 mM HEPES. This is due, in part, to potential cytotoxicity associated with this high level of HEPES. An approximately 30% loss in cell viability with the addition of 50 mM HEPES was determined by using the decreased conversion of 3-(4,5-dimethylthiazol-2-yl)-2,5-diphenyltetrazolium bromide (MTT) to formazan to infer cytotoxicity of the treatment in comparison with a 10 mM HEPES control. The decrease in permeability between 10 and 25 mM may be due to increased buffering capacity; however, it has also been shown that HEPES may play a role in increasing ATP concentration *in vitro,* which could possibly have a cascade effect to increase barrier properties.[58] All final culture conditions determined through optimization efforts are summarized in Table 1.

Due to the importance of limiting paracellular permeation in *in-vitro* BBB cell models, changes in permeation of five paracellular markers of various size – [^{14}C]-urea, [^{14}C]-mannitol, [^{14}C]-sucrose, [^{14}C]-PEG-4000 and [^{14}C]-inulin – were measured (Table 2). When comparing permeation through hCMEC/D3 monolayers to the coculture, all markers trended towards a reduction in paracellular permeation for the direct contact coculture. For the largest marker, PEG-4000, the reduction in permeability in the coculture was the smallest of all markers; however, this is not unexpected as permeation through the hCMEC/D3 monolayer was sufficiently slow and it is unlikely that further pore size reduction would lead to sizable changes in permeability. A similar story can be said of the smallest marker, urea. It is apparent that this model is still unable to prevent permeation of polar molecules in this very low molecular weight range. Although all changes in permeability were determined to be insignificant by the Mann–Whitney test, this is primarily due to the limitations of a small sample size ($n = 3$). The most significant decrease in permeability was seen for mannitol as determined by the *t*-test ($P < 0.01$) With further testing, it is possible to elucidate significant decreases in permeability in the direct contact coculture compared with the monoculture system.

The reproducibility of the direct contact coculture model is imperative to assess the utility of this model. The permeability of [^{14}C]-inulin was used to determine the repeatability of paracellular results across independent experiments.

Table 2 Comparison of molecular weight and molecular radii with apparent permeability of paracellular model compounds[63,64]

Markers	Molecular weight	Stokes radius (Å)	Hydrodynamic radius (Å)	P_{app} ($\times 10^{-5}$ cm/s)
Urea	60	1.7	1.8	2.43 ± 0.155
Mannitol	182	3.6	4.3	1.52 ± 0.069
Sucrose	342	4.6	5.2	1.17 ± 0.008
Inulin	5000	13.9	10	0.754 ± 0.030
PEG-4000	4000	16.4	15.9	0.357 ± 0.010

Although there is some difference between the permeability values obtained across multiple experiments, this is to be expected with slight variations in study conditions or cell passage number.

To investigate the impact of direct coculture, an indirect coculture with astrocytes on the basolateral side of the Transwell was also examined. As mentioned, it is often difficult to compare models between different laboratories due to differences in culture protocol, media selection, passaging and cell source.[49,50] Therefore, the indirect model was established under the same conditions and protocols as the direct contact coculture. As was hypothesized, a decrease in [^{14}C]-mannitol and [^{14}C]-sucrose apparent permeabilities was seen when the astrocytes were in direct cell contact, and determined to be significant by the *t*-test ($P < 0.05$). Further investigation is needed to determine the underlying factors leading to this increased tightness.

To assess passive transcellular permeation, the apparent permeability of [^{14}C]-propranolol was measured. Propranolol is often used as a passive transcellular marker due to its high octanol/water coefficient leading to almost exclusively transcellular permeation.[59] Due to the extra cell layer in the coculture model, it was expected that transcellular permeation would be reduced. While permeability was reduced in the coculture, changes between monoculture and coculture were not significant ($P > 0.05$). To further examine this discrepancy, [^{14}C]-propranolol permeability was also measured across human astrocyte monolayers and was found to be approximately threefold higher than hCMEC/D3 monolayers or the direct contact coculture. This finding validates the coculture permeability data as the hCMEC/D3 cell layer appears to be the rate-limiting barrier to permeation. While astrocytes do play a role in our model, it is unknown whether there is a significant contribution of paracellular flux for propranolol that may obfuscate transcellular permeation. While propranolol is unlikely to cross the tight junctions between endothelial cells, astrocyte endfeet are known to be much further apart with pores 20–30 Å wide *in vivo*, which may allow greater paracellular movement. Therefore, additional studies are required to understand differences between the apparent permeabilities for hCMEC/D3 and human astrocyte monocultures particularly to elucidate the mechanism of transport across the human astrocyte layer.

Efflux transporters are an important aspect of the BBB as it is a major line of defence to xenobiotics. Rhodamine 123 is a known P-gp substrate and is often used to determine functional expression of P-gp in BMEC cell lines.[8,17,60,61] Verapamil was used as a P-gp inhibitor to show the difference in total cellular accumulation of rhodamine 123 in its presence. The results of this study showed that rhodamine 123 accumulation is increased in both the monoculture and direct contact coculture models in the presence of verapamil, although there was no significant difference when compared with the absence of inhibitor. The lack of significance may be due to variations in P-gp expression as the hCMEC/D3 cell line increases in passage.[61] However, the total accumulation of rhodamine 123 both in the presence and in the absence of verapamil is greater in the hCMEC/D3 monoculture compared with the coculture, which may suggest that the level of functional efflux is higher when the hCMEC/D3 cells are in direct contact with astrocytes. Due to the nature of this model, with two cell types in direct contact, further experiments would be needed to fully assess the role that the astrocytes play in the transporter activity of the hCMEC/D3 cells.

Overall, this proof-of-concept study suggests direct contact coculture of human astrocytes and hCMEC/D3s leads to some tightening of the leaky tight junctions often found in hCMEC/D3 monoculture with minimal modification to other routes of permeation. While this model is still significantly leakier than *in-vivo* conditions, it represents an improvement in the paracellular leakage observed in many cell culture models and an advancement in physiologically relevant screening models for determining passive diffusion properties of drugs in the BBB. It should also be noted that while *in-vivo* tightness would be ideal, it may be unnecessary for drug screening. While current TEER values are much lower than found *in vivo*, it is possible that small changes in tight junction pore radii will lead to very large increases in TEER, as highlighted by Ho and colleagues.[47] Due to the nature of paracellular permeation, these large changes in TEER may have little effect on paracellular permeation due to the difference in the hydrodynamic size of ions being measured (sodium, potassium, calcium, chloride, magnesium, etc., vs drug molecules).[31,62] That is, NCEs targeted to the brain are often much larger and more lipophilic molecules than the ions whose movement across the cellular barrier determines TEER. In addition, the vast majority of all NCEs are not as small or polar as urea, mannitol or even sucrose. Moreover, TEER values can also be dramatically influenced by several other factors such as ionic strength, buffer variations and temperature that can be confounding variables.

Lastly, species differences are a major cofounder in translation of preclinical screening to humans. Differences in morphology, function and regulation are all common. As the common goal is to expedite human translation, it may be better in theory to use a slightly less restrictive human model than a tighter animal model for the screening and ranking of pharmaceutical molecules, provided the human model can discriminate between compounds in series. This will reduce some issues such as transport and enzyme affinities and capacities observed between species and better enable an assessment of transcellular permeation *in vivo* in humans.

Conclusion

As the occurrence of neurological diseases rise along with the number of druggable targets and compounds, a more relevant and robust *in-vitro* cell culture method has become of paramount importance for preclinical screening and lead candidate selection and optimization. The hCMEC/D3 cells have been shown to be functionally similar to primary brain endothelial cells; however, their main downfall has been the presence of leaky tight junctions. These leaky tight junctions obfuscate the delineation of transcellular routes of permeation of many compounds and potentially lead to inaccurate *in-vivo* predictions. Therefore, it is believed that reducing paracellular permeation to levels closer to that found *in vivo* may lead to a more robust BBB model.

Some promise has been shown in the reduction in paracellular permeability through coculture with astrocytes. However, current models often utilize indirect contact methods in which endothelial cells and astrocytes are separated by the Transwell®-permeable support. Here, it is shown that direct contact coculture of human astrocytes and hCMEC/D3 cells leads to a significant decrease in permeation of paracellular markers, as determined by the t-test. This methodology may serve as a better model for further optimization and *in-vivo* prediction. In addition, seeding of both cell types onto the apical chamber of the Transwell® is likely to be much more conducive to high-throughput screening. Though, further investigation including microscopy, transcriptomic and proteomic analysis and drug screening must be completed to confirm *in-vivo* relevancy; it is believed that this model is a step in the right direction for enhancing the ability to screen BBB permeation of neurotherapeutic and neurotoxic agents.

Declaration

Acknowledgements

The authors would like to acknowledge Drs. Pierre-Olivier Courad, Babbette Weksler and Ignacio Romero for providing the hCMEC/D3 cell line for these studies; Dr. Lori Karpes and Mr. Aimable Ngendahimana for their technical assistance with the project; and Ms. Monika Lavan for her technical critique of the manuscript. The authors would also like to acknowledge the financial support from the National Institute of General Medical Sciences (R01-GM65448) and Graduate Fellowship support through the Ross Fellowship, the Ronald Dollens' Graduate Scholarship and the Migliaccio/Pfizer Fellowship.

References

1. Abbott NJ. Blood-brain barrier structure and function and the challenges for CNS drug delivery. *J Inherit Metab Dis* 2013; 36: 437–449.
2. Abbott NJ. Astrocyte-endothelial interactions and blood-brain barrier permeability. *J Anat* 2002; 200: 629–638.
3. Ballabh P *et al.* The blood-brain barrier: an overview: structure, regulation, and clinical implications. *Neurobiol Dis* 2004; 16: 1–13.
4. Cecchelli R *et al.* Modelling of the blood-brain barrier in drug discovery and development. *Nat Rev Drug Discov* 2007; 6: 650–661.
5. Cohen-Kashi Malina K *et al.* Closing the gap between the in-vivo and in-vitro blood-brain barrier tightness. *Brain Res* 2009; 1284: 12–21.
6. Hatherell K *et al.* Development of a three-dimensional, all-human in vitro model of the blood-brain barrier using mono-, co-, and tri-cultivation Transwell models. *J Neurosci Methods* 2011; 199: 223–229.
7. Holash JA *et al.* Re-evaluating the role of astrocytes in blood-brain barrier induction. *Dev Dyn* 1993; 197: 14–25.
8. Poller B *et al.* The human brain endothelial cell line hCMEC/D3 as a human blood-brain barrier model for drug transport studies. *J Neurochem* 2008a; 107: 1358–1368.
9. Liebner S *et al.* Correlation of tight junction morphology with the expression of tight junction proteins in blood-brain barrier endothelial cells. *Eur J Cell Biol* 2000; 79: 707–717.
10. Wolburg H, Lippoldt A. Tight junctions of the blood-brain barrier: development, composition and regulation. *Vascul Pharmacol* 2002; 38: 323–337.
11. Schrade A *et al.* Expression and localization of claudins-3 and -12 in transformed human brain endothelium. *Fluids Barriers CNS* 2012; 9: 6.
12. On NH, Miller DW. Transporter-based delivery of anticancer drugs to the brain: improving brain penetration by minimizing drug efflux at the blood-brain barrier. *Curr Pharm Des* 2014; 20: 1499–1509.
13. Abbott NJ. Dynamics of CNS barriers: evolution, differentiation, and modulation. *Cell Mol Neurobiol* 2005; 25: 5–23.
14. Berezowski V *et al.* Contribution of glial cells and pericytes to the mRNA profiles of P-glycoprotein and multidrug resistance-associated proteins in an in vitro model of the blood-brain barrier. *Brain Res* 2004; 1018: 1–9.
15. Engelhardt B. Development of the blood-brain barrier. *Cell Tissue Res* 2003; 314: 119–129.
16. Schiera G *et al.* Synergistic effects of neurons and astrocytes on the differentiation of brain capillary endothelial cells in culture. *J Cell Mol Med* 2003; 7: 165–170.
17. Lippmann ES *et al.* Derivation of blood-brain barrier endothelial cells from human pluripotent stem cells. *Nat Biotechnol* 2012; 30: 783–791.
18. Meyer RP *et al.* Possible function of astrocyte cytochrome P450 in control of xenobiotic phenytoin in the brain: in vitro studies on murine astrocyte primary cultures. *Exp Neurol* 2001; 167: 376–384.

19. Cohen MP *et al.* Collagen production by cultured retinal capillary pericytes. *Invest Ophthalmol Vis Sci* 1980; 19: 90–94.
20. Hirschi KK, D'Amore PA. Pericytes in the microvasculature. *Cardiovasc Res* 1996; 32: 687–698.
21. Mandarino LJ *et al.* Regulation of fibronectin and laminin synthesis by retinal capillary endothelial cells and pericytes in vitro. *Exp Eye Res* 1993; 57: 609–621.
22. Cecchelli R *et al.* In vitro model for evaluating drug transport across the blood-brain barrier. *Adv Drug Deliv Rev* 1999; 36: 165–178.
23. Dehouck MP *et al.* An easier, reproducible, and mass-production method to study the blood-brain barrier in vitro. *J Neurochem* 1990; 54: 1798–1801.
24. Deli MA *et al.* Permeability studies on in vitro blood-brain barrier models: physiology, pathology, and pharmacology. *Cell Mol Neurobiol* 2005; 25: 59–127.
25. Demeuse P *et al.* Compartmentalized coculture of rat brain endothelial cells and astrocytes: a syngenic model to study the blood-brain barrier. *J Neurosci Methods* 2002;121:21–31.
26. Di L *et al.* High throughput artificial membrane permeability assay for blood-brain barrier. *Eur J Med Chem* 2003; 38: 223–232.
27. Eigenmann DE *et al.* Comparative study of four immortalized human brain capillary endothelial cell lines, hCMEC/D3, hBMEC, TY10, and BB19, and optimization of culture conditions, for an in vitro blood-brain barrier model for drug permeability studies. *Fluids Barriers CNS* 2013; 10: 33.
28. Gaillard PJ *et al.* Establishment and functional characterization of an in vitro model of the blood-brain barrier, comprising a co-culture of brain capillary endothelial cells and astrocytes. *Eur J Pharm Sci* 2001; 12: 215–222.
29. Jeliazkova-Mecheva VV, Bobilya DJ. A porcine astrocyte/endothelial cell coculture model of the blood-brain barrier. *Brain Res Brain Res Protoc* 2003; 12: 91–98.
30. Kido Y *et al.* Evaluation of blood-brain barrier transporters by co-culture of brain capillary endothelial cells with astrocytes. *Drug Metab Pharmacokinet* 2002; 17: 34–41.
31. Sorensen M *et al.* The effect of beta-turn structure on the permeation of peptides across monolayers of bovine brain microvessel endothelial cells. *Pharm Res* 1997; 14: 1341–1348.
32. Weksler B *et al.* The hCMEC/D3 cell line as a model of the human blood brain barrier. *Fluids Barriers CNS* 2013; 10: 16.
33. Audus KL, Borchardt RT. Bovine brain microvessel endothelial cell monolayers as a model system for the blood-brain barrier. *Ann N Y Acad Sci* 1987; 507: 9–18.
34. Raub TJ *et al.* Permeability of bovine brain microvessel endothelial cells in vitro: barrier tightening by a factor released from astroglioma cells. *Exp Cell Res* 1992; 199: 330–340.
35. Weksler BB *et al.* Blood-brain barrier-specific properties of a human adult brain endothelial cell line. *FASEB J* 2005; 19: 1872–1874.
36. Carl SM *et al.* ABC and SLC transporter expression and pot substrate characterization across the human CMEC/D3 blood-brain barrier cell line. *Mol Pharm* 2010; 7: 1057–1068.
37. Vu K *et al.* Immortalized human brain endothelial cell line HCMEC/D3 as a model of the blood-brain barrier facilitates in vitro studies of central nervous system infection by Cryptococcus neoformans. *Eukaryot Cell* 2009; 8: 1803–1807.
38. Butt AM *et al.* Electrical resistance across the blood-brain barrier in anaesthetized rats: a developmental study. *J Physiol* 1990; 429: 47–62.
39. Siddharthan V *et al.* Human astrocytes/astrocyte-conditioned medium and shear stress enhance the barrier properties of human brain microvascular endothelial cells. *Brain Res* 2007; 1147: 39–50.
40. Garcia CM *et al.* Endothelial cell-astrocyte interactions and TGF beta are required for induction of blood-neural barrier properties. *Brain Res Dev Brain Res* 2004; 152: 25–38.
41. Frum Y *et al.* Evidence that drug flux across synthetic membranes is described by normally distributed permeability coefficients. *Eur J Pharm Biopharm* 2007; 67: 434–439.
42. Khan GM *et al.* Assessment of drug permeability distributions in two different model skins. *Int J Pharm* 2005; 303: 81–87.
43. Forster C *et al.* Differential effects of hydrocortisone and TNFalpha on tight junction proteins in an in vitro model of the human blood-brain barrier. *J Physiol* 2008a; 586: 1937–1949.
44. Paolinelli R *et al.* Wnt activation of immortalized brain endothelial cells as a tool for generating a standardized model of the blood brain barrier in vitro. *PLoS ONE* 2013; 8: 11.
45. van Noort M *et al.* Wnt signaling controls the phosphorylation status of beta-catenin. *J Biol Chem* 2002; 277: 17901–17905.
46. Zougbede S *et al.* Metabolic acidosis induced by Plasmodium falciparum intraerythrocytic stages alters blood-brain barrier integrity. *J Cereb Blood Flow Metab* 2011; 31: 514–526.
47. Adson A *et al.* Quantitative approaches to delineate paracellular diffusion in cultured epithelial cell monolayers. *J Pharm Sci* 1994; 83: 1529–1536.
48. Knipp GT *et al.* Paracellular diffusion in Caco-2 cell monolayers: effect of perturbation on the transport of hydrophilic compounds that vary in charge and size. *J Pharm Sci* 1997a; 86: 1105–1110.
49. Roth WJ *et al.* The effects of intralaboratory modifications to media composition and cell source on the expression of pharmaceutically relevant transporters and metabolizing genes in the Caco-2 cell line. *J Pharm Sci* 2012; 101: 3962–3978.
50. Lindley DJ *et al.* The effects of media on pharmaceutically relevant transporters in the human HT-29 adenocarcinoma cell line: does culture media need to be controlled? *J Pharm Sci* 2012; 101: 1616–1630.
51. Helms HC *et al.* Paracellular tightness and claudin-5 expression is increased in the BCEC/astrocyte blood-brain

barrier model by increasing media buffer capacity during growth. *AAPS J* 2010; 12: 759–770.
52. Wolburg H *et al.* Modulation of tight junction structure in blood-brain barrier endothelial cells. Effects of tissue culture, second messengers and cocultured astrocytes. *J Cell Sci* 1994; 107 (Pt 5): 1347–1357.
53. Urich E *et al.* Transcriptional profiling of human brain endothelial cells reveals key properties crucial for predictive in vitro blood-brain barrier models. *PLoS ONE* 2012; 7: e38149.
54. Li G *et al.* Permeability of endothelial and astrocyte cocultures: in vitro blood-brain barrier models for drug delivery studies. *Ann Biomed Eng* 2010; 38: 2499–2511.
55. Abbott NJ *et al.* Astrocyte-endothelial interactions at the blood-brain barrier. *Nat Rev Neurosci* 2006; 7: 41–53.
56. Arthur FE *et al.* Astrocyte-mediated induction of tight junctions in brain capillary endothelium: an efficient in vitro model. *Brain Res* 1987; 433: 155–159.
57. Lippmann ES *et al.* Modeling the blood-brain barrier using stem cell sources. *Fluids Barriers CNS* 2013; 10: 2.
58. Luo SH *et al.* Effect of HEPES buffer on the uptake and transport of P-glycoprotein substrates and large neutral amino acids. *Mol Pharm* 2010; 7: 412–420.
59. Pade V, Stavchansky S. Estimation of the relative contribution of the transcellular and paracellular pathway to the transport of passively absorbed drugs in the Caco-2 cell culture model. *Pharm Res* 1997; 14: 1210–1215.
60. Lippmann ES *et al.* A retinoic acid-enhanced, multicellular human blood-brain barrier model derived from stem cell sources. *Sci Rep* 2014; 4: 4160.
61. Tai LM *et al.* Polarized P-glycoprotein expression by the immortalised human brain endothelial cell line, hCMEC/D3, restricts apical-to-basolateral permeability to rhodamine 123. *Brain Res* 2009; 1292: 14–24.
62. Knipp GT *et al.* The effect of beta-turn structure on the passive diffusion of peptides across Caco-2 cell monolayers. *Pharm Res* 1997b; 14: 1332–1340.
63. Ghandehari H *et al.* Size-dependent permeability of hydrophilic probes across rabbit colonic epithelium. *J Pharmacol Exp Ther* 1997; 280: 747–753.
64. Schultz SG, Solomon AK. Determination of the effective hydrodynamic radii of small molecules by viscometry. *J Gen Physiol* 1961; 44: 1189–1199.